

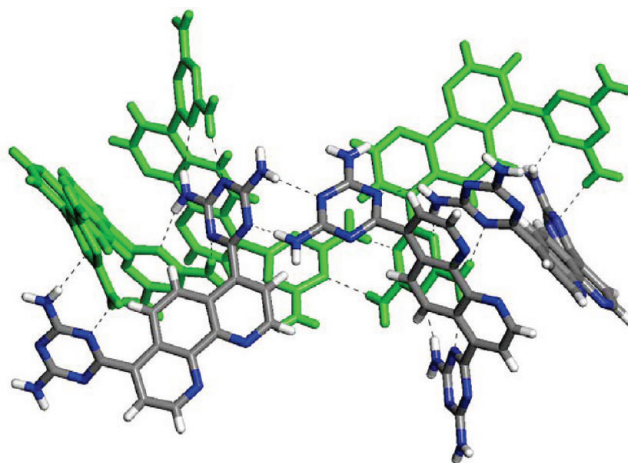
## Syntheses and Structures of Isomeric Diaminotriazinyl-Substituted 2,2'-Bipyridines and 1,10-Phenanthrolines

Adam Duong, Thierry Maris, Olivier Lebel,<sup>†</sup> and James D. Wuest\*

Département de Chimie, Université de Montréal, Montréal, Québec H3C 3J7, Canada

james.d.wuest@umontreal.ca

Received November 4, 2010

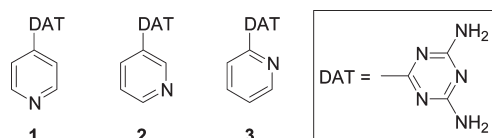


Isomeric 2,2'-bipyridines **4a–6a** and 1,10-phenanthrolines **7a–9a** with two diaminotriazinyl (DAT) substituents were synthesized to explore their dual ability to direct association by the chelation of metals and the characteristic hydrogen bonding of DAT groups. Crystals of compounds **4a–6a** and **7a–9a** were grown under diverse conditions, and their structures were solved by X-ray crystallography. Analysis revealed multiple shared features analogous to those observed in the structures of simpler DAT-substituted pyridines **1–3**. For example, the bipyridines and phenanthrolines favor flattened conformations except in the cases of compounds **8a** and **9a**, where the patterns of substitution prevent the DAT groups from lying in the plane of the phenanthroline core. As expected, the DAT groups form approximately coplanar hydrogen bonds according to standard motifs **I–III**, which play a key role in directing molecular organization. However, the structures of simple pyridines **1–3**, which favor efficiently packed chains and sheets, differ predictably from those of bipyridines **4a–6a** and phenanthrolines **7a–9a** in two ways: (1) The larger number of DAT groups in compounds **4a–9a** typically leads to complex three-dimensional networks held together by a larger number of hydrogen bonds per molecule, and (2) the need to respect multiple directional interactions prevents compounds **4a–9a** from forming closely packed structures, and significant quantities of guests are included. Together, these observations confirm the effectiveness of incorporating special groups such as DAT within more complex molecular structures to control association according to reliable patterns. Bipyridines **4a–6a** and phenanthrolines **7a–9a** promise to be particularly rich sources of new supramolecular chemistry because they have well-defined molecular topologies and a dual ability to direct association by chelating metals and by engaging in multiple hydrogen bonds according to reliable patterns.

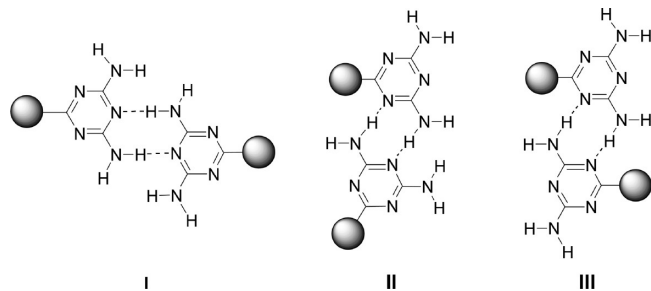
<sup>†</sup> Fellow of the Ministère de l'Éducation du Québec, 2002–2004.

## Introduction

Isomeric diaminotriazinyl-substituted pyridines **1–3** form a family of compounds with diverse properties of interest. In particular, the dual presence of diaminotriazinyl (DAT) and pyridyl groups creates a significant potential for association controlled by hydrogen bonds,<sup>1</sup> aromatic interactions, and coordination to metals.<sup>2–6</sup> As a result, such compounds are well designed to serve as components of ordered molecular structures created by design, such as three-dimensional crystals or two-dimensional networks adsorbed on surfaces. In addition, such compounds and their complexes have potential applications in biological science; for example, they show promise in cancer chemotherapy as cytotoxic DNA-metallointercalators,<sup>3</sup> and they are also effective insect chemosterilants and larvicides.<sup>7</sup>

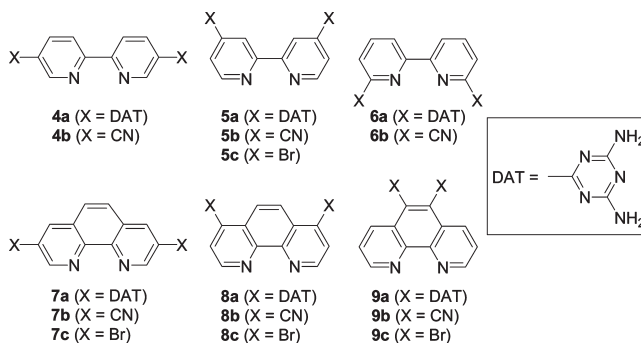


To provide a deeper understanding of the associative properties of such compounds, we have recently reported the structures of DAT-substituted pyridines **1–3** and various analogues.<sup>8</sup> Comparison of the structures revealed significant underlying similarities. Specifically, the compounds tend to adopt predictably flattened conformations,<sup>1</sup> and they form approximately coplanar hydrogen bonds according to motifs characteristic of DAT groups, as defined by isomeric supramolecular homosynthons **I–III**.<sup>1,9</sup> These interactions



play a dominant role in directing molecular organization in the crystalline state. Together, the flattened molecular topologies and the shared presence of a dominant site of association ensure that compounds **1–3** and simple analogues crystallize in related ways to give structures that feature chains, tapes,

and layers. In certain cases, in fact, the molecular organization adopted by different DAT-substituted pyridines was found to be virtually identical, even when the orientation of the pyridyl group was changed. These observations show that the DAT group has a special ability to control aggregation by forming multiple directional intermolecular interactions according to reliable patterns. This suggests that the group can be incorporated within more complex molecular structures to determine how association will occur.



The intriguing behavior of relatively simple DAT-substituted pyridines **1–3** encouraged us to study two sets of more complex relatives, isomeric DAT-substituted 2,2'-bipyridines **4a–6a** and 1,10-phenanthrolines **7a–9a**. By offering well-defined molecular structures, combined with the ability of DAT groups to direct association by hydrogen bonding and with the capacity of 2,2'-bipyridines and 1,10-phenanthrolines to chelate metals,<sup>10</sup> compounds **4a–9a** promise to be rich sources of new supramolecular chemistry. Syntheses and structures of these compounds are reported below to provide a foundation for future studies.

## Results and Discussion

**Syntheses of Isomeric DAT-Substituted 2,2'-Bipyridines **4a–6a** and 1,10-Phenanthrolines **7a–9a**.** Bipyridines **4a**, **5a**, and **6a** were prepared from the corresponding dinitriles **4b**,<sup>11–13</sup> **5b**,<sup>13–15</sup> and **6b**,<sup>15,16</sup> respectively, by heating with dicyandiamide and KOH under standard conditions.<sup>17</sup> Phenanthrolines **7a**, **8a**, and **9a** were synthesized in an analogous way from dinitriles **7b**, **8b**,<sup>18</sup> and **9b**, respectively. Yields of DAT-substituted compounds **4a–8a** were all excellent

(1) For recent references, see: Maly, K. E.; Gagnon, E.; Maris, T.; Wuest, J. D. *J. Am. Chem. Soc.* **2007**, *129*, 4306–4322.

(2) Zhao, Q.-H.; Fan, A.-L.; Li, L.-N.; Xie, M.-J. *Acta Crystallogr.* **2009**, *E65*, m622.

(3) Ma, D.-L.; Che, C.-M. *Chem.—Eur. J.* **2003**, *9*, 6133–6144.

(4) Chan, C.-W.; Mingos, D. M. P.; White, A. J. P.; Williams, D. J. *Polyhedron* **1996**, *15*, 1753–1767.

(5) Diehl, H.; Buchanan, E. B., Jr.; Smith, G. F. *Anal. Chem.* **1960**, *32*, 1117–1119.

(6) Case, F. H.; Koft, E. *J. Am. Chem. Soc.* **1959**, *81*, 905–906.

(7) DeMilo, A. B.; Bořkovec, A. B.; Cohen, C. F.; Robbins, W. E. *J. Agric. Food Chem.* **1981**, *29*, 82–84.

(8) Duong, A.; Maris, T.; Wuest, J. D. *Cryst. Growth Des.* **2011**, *11*, 287–294.

(9) Nangia, A.; Desiraju, G. R. *Top. Curr. Chem.* **1998**, *198*, 57–95. Desiraju, G. R. *Angew. Chem., Int. Ed.* **1995**, *34*, 2311–2327.

(10) For a recent review, see: Ye, B.-H.; Tong, M.-L.; Chen, X.-M. *Coord. Chem. Rev.* **2005**, *249*, 545–565.

(11) Veauthier, J. M.; Carlson, C. N.; Collis, G. E.; Kiplinger, J. L.; John, K. D. *Synthesis* **2005**, 2683–2686.

(12) Wu, H.-P.; Janiak, C.; Rheinwald, G.; Lang, H. *J. Chem. Soc., Dalton Trans.* **1999**, 183–190. Janiak, C.; Deblon, S.; Wu, H.-P. *Synth. Commun.* **1999**, *29*, 3341–3352. Pichot, F.; Beck, J. H.; Elliott, C. M. *J. Phys. Chem. A* **1999**, *103*, 6263–6267. Whittle, C. P. *J. Heterocycl. Chem.* **1977**, *14*, 191–194.

(13) Baxter, P. N. W.; Connor, J. A. *J. Organomet. Chem.* **1988**, *355*, 193–196.

(14) Losse, S.; Görls, H.; Groarke, R.; Vos, J. G.; Rau, S. *Eur. J. Inorg. Chem.* **2008**, 4448–4452.

(15) Stanek, J.; Caravatti, G.; Capraro, H.-G.; Furet, P.; Mett, H.; Schneider, P.; Regenass, U. *J. Med. Chem.* **1993**, *36*, 46–54.

(16) Mukkala, V.-M.; Kwiatkowski, M.; Kankare, J.; Takalo, H. *Helv. Chim. Acta* **1993**, *76*, 893–899. Baxter, P. N. W.; Connor, J. A.; Schweizer, W. B.; Wallis, J. D. *J. Chem. Soc., Dalton Trans.* **1992**, 3015–3019. Burstall, F. H. *J. Chem. Soc.* **1938**, 1662–1672.

(17) Simons, J. K.; Saxton, M. R. *Organic Syntheses*; Wiley: New York, 1963; Collect. Vol. IV, p 78.

(18) Goossen, L. J.; Rodriguez, N.; Linder, C.; Lange, P. P.; Fromm, A. *ChemCatChem* **2010**, *2*, 430–442.

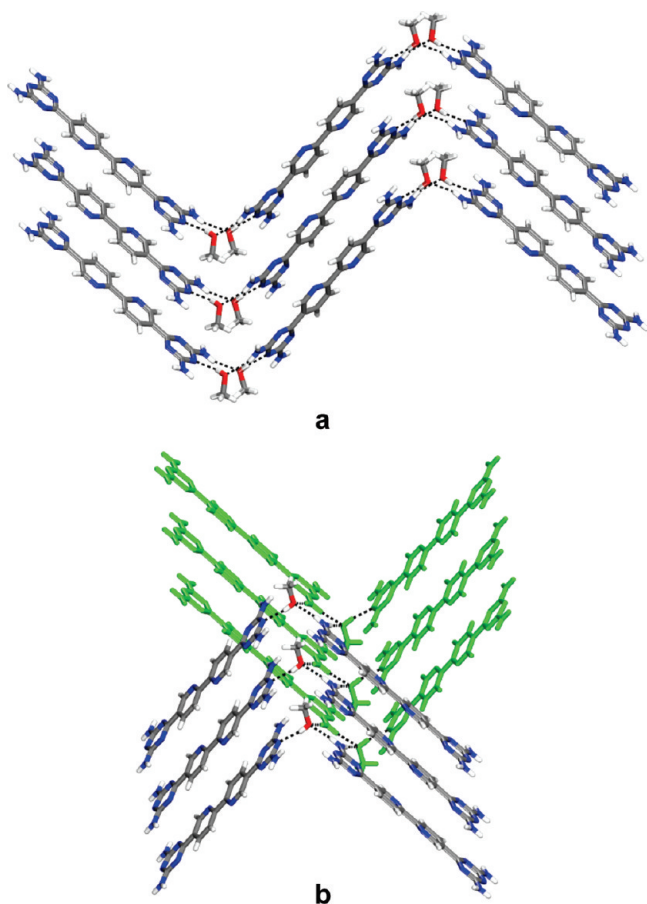


**FIGURE 1.** Views of the structure of crystals of the 1:2 solvate of DAT-substituted bipyridine **4a** with MeOH. (a) View showing how hydrogen bonding according to a variant of motif **I** with intervening molecules of MeOH produces chains and how the chains stack to produce layers. Hydrogen bonds are represented by broken lines, and carbon atoms are shown in gray, hydrogen atoms in white, nitrogen atoms in blue, and oxygen atoms in red. (b) View showing hydrogen bonding between two adjacent layers, with one layer highlighted in green.

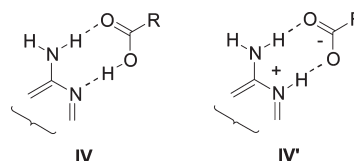
(85–90%), but *ortho*-disubstituted phenanthroline **9a** was obtained in only 20% yield. Other arenes with adjacent DAT groups have been prepared by the normal method,<sup>19</sup> so we attribute the poor yield of phenanthroline **9a** to the high degree of substitution of the central ring.

Dinitrile precursor **4b** was made from the corresponding dibromide as reported by John et al.,<sup>11</sup> and isomeric dinitrile **6b** was obtained by a modified Reissert–Henze reaction, as described by Stanek et al.<sup>15</sup> Known dinitrile **5b** was prepared by a new route in 63% yield from dibromide **5c**<sup>20</sup> by applying the catalytic methodology of John et al.<sup>11</sup> This procedure was also used to convert 3,8-dibromo-1,10-phenan-

throline (**7c**),<sup>21</sup> 4,7-dibromo-1,10-phenanthroline (**8c**),<sup>22</sup> and 5,6-dibromo-1,10-phenanthroline (**9c**)<sup>23</sup> into dinitriles **7b–9b**, respectively, in good yields (52–62%).

**Structure of Crystals of DAT-Substituted 2,2'-Bipyridine 4a.** Compound **4a** proved to have low solubility in most organic solvents, but crystals suitable for X-ray diffraction could be grown from DMSO/MeOH and H<sub>2</sub>O/CF<sub>3</sub>COOH (TFA). Crystals obtained from DMSO/MeOH were found to belong to the monoclinic space group *P2<sub>1</sub>/c* and to have the composition **4a**·2MeOH. Views of the structure are provided in Figure 1, and other crystallographic data are presented in Table 1. As expected, the bipyridyl core of compound **4a** adopts an essentially coplanar *anti* conformation (dihedral angle = 0.0°),<sup>24</sup> and the DAT groups lie close to the plane of the core. Molecules associate to form zigzag chains by hydrogen bonding according to a variant of synthon **I**, with intervening molecules of MeOH (Figure 1a). In the intra-chain hydrogen bonds, the O–H···N and N–H···O distances have normal values (2.772 and 2.960 Å, respectively). Face-to-face aromatic interactions of the chains direct the formation of layers, which are linked to form the ultimate three-dimensional structure by various interlayer interactions (Figure 1b), including N–H···N(pyridine) hydrogen bonds (2.976 Å) and N–H···O hydrogen bonds (2.960 Å and 2.998 Å).

Crystals of DAT-substituted bipyridine **4a** grown from TFA/H<sub>2</sub>O proved to belong to the monoclinic space group *P2<sub>1</sub>/c* and to have the composition **4a**·2TFA·H<sub>2</sub>O. Figure 2 provides a view of the proposed structure, and Table 1 presents other crystallographic data. The bipyridyl core adopts a twisted *anti* conformation (dihedral angle = 32.1°), but each pyridyl ring and its DAT substituent are nearly coplanar. The proposed structure (Figure 2) shows that both DAT groups are engaged in hydrogen bonding with TFA according to a variant of standard heterosynthon **IV**, with full



proton transfer (**IV'**).<sup>25–28</sup> Each molecule of doubly protonated compound **4a** is joined to two neighbors to form tapes by a total of four N–H···N(pyridine) hydrogen bonds

(23) Feng, M.; Chan, K. S. *Organometallics* **2002**, *21*, 2743–2750.

(24) For recent references, see: Chein, R.-J.; Corey, E. J. *Org. Lett.* **2010**, *12*, 132–135. Zahn, S.; Reckien, W.; Kirchner, B.; Staats, H.; Matthey, J.; Lützen, A. *Chem.—Eur. J.* **2009**, *15*, 2572–2580. Amarante, T. R.; Figueiredo, S.; Lopes, A. D.; Gonçalves, I. S.; Almeida Paz, F. A. *Acta Crystallogr.* **2009**, *E65*, o2047.

(25) For recent references, see: Singh, D.; Bhattacharyya, P. K.; Baruah, J. B. *Cryst. Growth Des.* **2010**, *10*, 348–356. Shattock, T. R.; Arora, K. K.; Vishweshwar, P.; Zaworotko, M. J. *Cryst. Growth Des.* **2008**, *8*, 4533–4545. Babu, N. J.; Nangia, A. *Cryst. Growth Des.* **2006**, *6*, 1995–1999. Aakeröy, C. B.; Desper, J.; Urbina, J. F. *CrystEngComm* **2005**, *7*, 193–201. Dale, S. H.; Elsegood, M. R. J.; Hemmings, M.; Wilkinson, A. L. *CrystEngComm* **2004**, *6*, 207–214.

(26) The large difference between the pK<sub>a</sub> value of TFA (pK<sub>a</sub> 0.5) and those of the conjugate acids of pyridine (pK<sub>a</sub> 5.2) or aminotriazines such as melamine (pK<sub>a</sub> 5)<sup>27</sup> provides a substantial driving force for proton transfer.<sup>28</sup>

(27) Jang, Y. H.; Hwang, S.; Chang, S. B.; Ku, J.; Chung, D. S. *J. Phys. Chem. A* **2009**, *113*, 13036–13040.

(28) For discussion, see: He, G.; Chow, P. S.; Tan, R. B. H. *Cryst. Growth Des.* **2009**, *9*, 4529–4532. Mohamed, S.; Tocher, D. A.; Vickers, M.; Karamertzanis, P. G.; Price, S. L. *Cryst. Growth Des.* **2009**, *9*, 2881–2889. Childs, S. L.; Stahly, G. P.; Park, A. *Mol. Pharmaceutics* **2007**, *4*, 323–338. Bhogala, B. R.; Basavoju, S.; Nangia, A. *CrystEngComm* **2005**, *7*, 551–562.

(19) Díaz-Ortiz, Á.; Elguero, J.; Foces-Foces, C.; de la Hoz, A.; Moreno, A.; del Carmen Mateo, M.; Sánchez-Migallón, A.; Valiente, G. *New J. Chem.* **2004**, *28*, 952–958. Mackenzie, S. M.; Stevens, M. F. G. *J. Chem. Soc. C* **1970**, 2298–2308. Iwakura, Y.; Uno, K.; Shiraishi, S. *Bull. Chem. Soc. Jpn.* **1965**, *38*, 1820–1824.

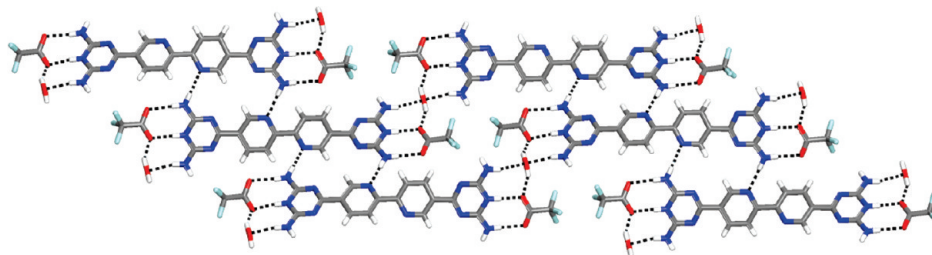
(20) Carlson, B.; Phelan, G. D.; Kaminsky, W.; Dalton, L.; Jiang, X.; Liu, S.; Jen, A. K.-Y. *J. Am. Chem. Soc.* **2002**, *124*, 14162–14172.

(21) Saitoh, Y.; Koizumi, T.-a.; Osakada, K.; Yamamoto, T. *Can. J. Chem.* **1997**, *75*, 1336–1339.

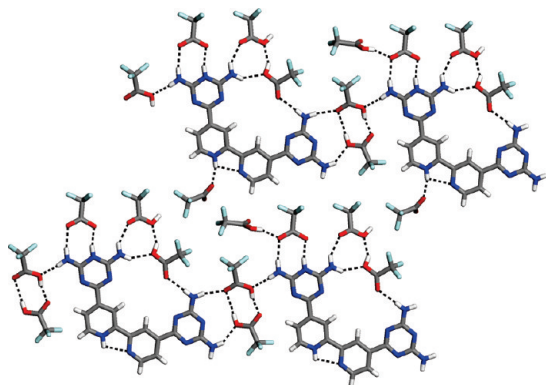
(22) Graf, G. I.; Hastreiter, D.; Everson da Silva, L.; Andrade Rebelo, R.; Garrido Montalban, A.; McKillop, A. *Tetrahedron* **2002**, *58*, 9095–9100.

TABLE 1. Crystallographic Data for Isomeric DAT-Substituted Bipyridines 4a–6a

	4a · 2MeOH	4a · 2TFA · H <sub>2</sub> O	5a · 7TFA	6a · 2DMSO
crystallization medium	DMSO/MeOH	TFA/H <sub>2</sub> O	TFA/H <sub>2</sub> O	DMSO/CH <sub>2</sub> Cl <sub>2</sub>
formula	C <sub>18</sub> H <sub>22</sub> N <sub>12</sub> O <sub>2</sub>	C <sub>20</sub> H <sub>18</sub> F <sub>6</sub> N <sub>12</sub> O <sub>5</sub>	C <sub>30</sub> H <sub>21</sub> F <sub>21</sub> N <sub>12</sub> O <sub>14</sub>	C <sub>20</sub> H <sub>26</sub> N <sub>12</sub> O <sub>2</sub> S <sub>2</sub>
crystal system	monoclinic	monoclinic	monoclinic	monoclinic
space group	<i>P</i> 2 <sub>1</sub> / <i>c</i>	<i>P</i> 2 <sub>1</sub> / <i>c</i>	<i>P</i> 2 <sub>1</sub> / <i>c</i>	<i>P</i> 2 <sub>1</sub> / <i>c</i>
<i>a</i> (Å)	15.4348(4)	17.4190(17)	18.1219(19)	7.9366(2)
<i>b</i> (Å)	5.1653(2)	7.4383(7)	15.1818(15)	16.990(1)
<i>c</i> (Å)	12.6502(3)	19.102(2)	17.9876(16)	19.563(1)
$\alpha$ (deg)	90	90	90	90
$\beta$ (deg)	95.858(1)	107.558(5)	119.092(4)	113.204(9)
$\gamma$ (deg)	90	90	90	90
<i>V</i> (Å <sup>3</sup> )	1003.3(1)	2359.7(4)	4325.7(7)	2424.5(5)
<i>Z</i>	2	4	4	4
$\rho_{\text{calc}}$ (g cm <sup>−3</sup> )	1.451	1.746	1.801	1.454
<i>T</i> (K)	100	150	100	100
$\mu$ (mm <sup>−1</sup> )	0.861	1.423	1.803	2.382
<i>R</i> <sub>1</sub> , <i>I</i> > 2 $\sigma$ ( <i>I</i> )	0.0446	0.0616	0.0689	0.0541
<i>R</i> <sub>1</sub> , all data	0.0456	0.0739	0.0779	0.0544
<i>wR</i> <sub>2</sub> , <i>I</i> > 2 $\sigma$ ( <i>I</i> )	0.1381	0.1406	0.1633	0.1278
<i>wR</i> <sub>2</sub> , all data	0.1396	0.1425	0.1784	0.1279
independent reflections	1791	3061	7988	4402
observed reflections [ <i>I</i> > 2 $\sigma$ ( <i>I</i> )]	1681	1601	5352	4356



**FIGURE 2.** View of the structure of crystals of the 1:2:1 solvate of DAT-substituted bipyridine **4a** with TFA and H<sub>2</sub>O. The view shows how doubly protonated compound **4a** forms hydrogen bonds according to standard motif IV', how tapes are produced by additional N–H···N-(pyridine) hydrogen bonds, and how the tapes are further linked by molecules of H<sub>2</sub>O to give sheets. Hydrogen bonds are represented by broken lines, and carbon atoms are shown in gray, hydrogen atoms in white, fluorine atoms in light blue, nitrogen atoms in dark blue, and oxygen atoms in red.



**FIGURE 3.** View of the structure of crystals of the 1:7 solvate of DAT-substituted bipyridine **5a** with TFA. The view shows that molecules of the doubly protonated form of compound **5a** are prevented from entering into direct contact by surrounding hydrogen-bonded TFA. Hydrogen bonds are represented by broken lines, and carbon atoms are shown in gray, hydrogen atoms in white, fluorine atoms in light blue, nitrogen atoms in dark blue, and oxygen atoms in red.

(average distance = 2.972 Å), reinforced by various C–H···N and C–H···O interactions (Figure 2).<sup>29,30</sup> Additional hydrogen bonds involving H<sub>2</sub>O link the tapes to form corrugated sheets (Figure 2), which stack to generate the full three-dimensional structure.<sup>31</sup> Surprisingly, the pyr-

idyl nitrogen atoms of compound **4a** are not protonated by TFA to give a salt, despite the potential exothermicity of this process.<sup>26–28</sup> It is possible that the N–H···N(pyridine) hydrogen-bonding motif of neighboring molecules (Figure 2) is favorable enough to engage the pyridyl nitrogen atoms and prevent their protonation by TFA.

**Structure of Crystals of Isomeric DAT-Substituted 2,2'-Bipyridine 5a.** Crystals of isomeric DAT-substituted bipyridine **5a** grown from TFA/H<sub>2</sub>O were found to belong to the monoclinic space group *P*2<sub>1</sub>/*c* and to have the composition **5a** · 7TFA. A view of the proposed structure appears in Figure 3, and other crystallographic data are provided in Table 1. The bipyridyl core of compound **5a** unexpectedly adopts a nearly coplanar *syn* conformation (dihedral angle = 2.2°), and each DAT substituent lies essentially in the plane of the core (Figure 3). In the structure shown in Figure 3, a DAT group is protonated by TFA according to motif IV', and the preference for a *syn* conformation is rationalized by proposing that a pyridyl nitrogen atom is also protonated by TFA.<sup>26–28</sup> Molecules of the doubly protonated form of compound **5a** are not in direct contact but

(29) Desiraju, G. R.; Steiner, T., *The Weak Hydrogen Bond in Structural Chemistry and Biology*; Oxford University Press: Oxford, U.K., 1999.

(30) For a review of C–H···O interactions, see: Desiraju, G. R. *Chem. Commun.* **2005**, 2995–3001.

(31) See the Supporting Information for details.

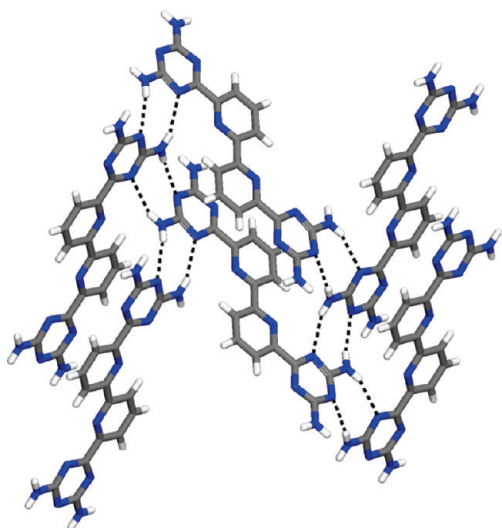


**FIGURE 4.** View of robust hydrogen-bonded layer in the structure of crystals of the 1:2 solvate of DAT-substituted bipyridine **6a** with DMSO. Hydrogen bonds are represented by broken lines, and carbon atoms are shown in gray, hydrogen atoms in white, and nitrogen atoms in blue. Molecules of DMSO are omitted for clarity.

are instead virtually surrounded by hydrogen-bonded TFA (Figure 3).

**Structure of Crystals of Isomeric DAT-Substituted 2,2'-Bipyridine 6a.** Crystals of DAT-substituted bipyridine **6a** grown from DMSO/CH<sub>2</sub>Cl<sub>2</sub> proved to belong to the monoclinic space group *P*2<sub>1</sub>/*c* and to have the composition **6a** • 2 DMSO. Figure 4 provides a view of the structure, and Table 1 summarizes other crystallographic data. As usual, the bipyridyl core of compound **6a** favors a nearly coplanar *anti* conformation (dihedral angle = 0.0°), and the DAT substituents lie close to the same plane (Figure 4). Each DAT group participates in four N–H···N(triazine) hydrogen bonds of type **II** (average distance = 3.162 Å), leading to the construction of robust layers in which each molecule of compound **6a** is linked to four neighbors by a total of eight hydrogen bonds (Figure 4). Molecular organization in the resulting layers is closely analogous to that observed in certain structures of simpler analogs **1–3** and their relatives.<sup>8</sup> Adjacent layers are separated by included molecules of DMSO,<sup>31</sup> which form N–H···O hydrogen bonds (average distance = 3.037 Å) with nearby DAT groups.

Crystallization of simple DAT-substituted pyridines **1–3** and their relatives has been shown to be controlled primarily by their flattened molecular topologies and by the ability of DAT groups to direct the formation of coplanar hydrogen bonds of types **I–III**.<sup>8</sup> As a result, these compounds typically crystallize in similar ways to give structures that incorporate chains, tapes, and layers. More complex DAT-substituted bipyridines **4a–6a** have the same key features, including a preference for flattened conformations and multiple DAT groups, so their behavior should be analogous. Indeed, both compounds **4a** and **6a** crystallize under selected conditions to give layered structures built from nearly planar conformers that engage in hydrogen bonding according to motifs **I–III** or similar patterns. In contrast, crystals of compounds **4a** and **5a** grown from TFA/H<sub>2</sub>O have largely unrelated structures. This inconsistency can be attributed to the ability of TFA to protonate DAT groups and thereby disrupt their

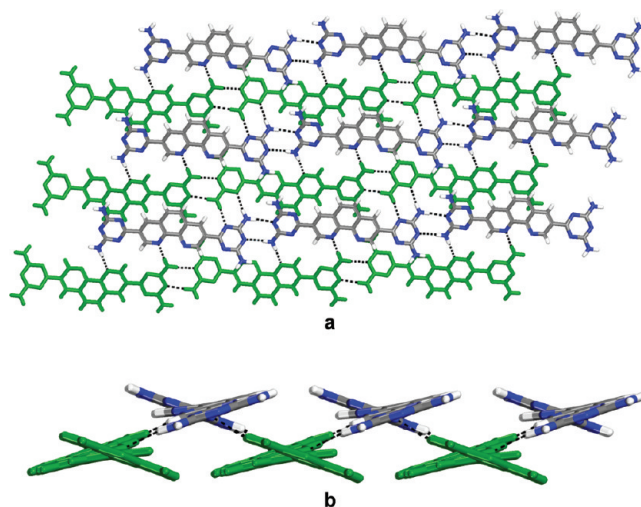


**FIGURE 5.** Views of the structure of crystals of the 1:2:1 solvate of DAT-substituted phenanthroline **7a** with DMSO and CHCl<sub>3</sub>. Hydrogen bonds are represented by broken lines, and carbon atoms are shown in gray, hydrogen atoms in white, and nitrogen atoms in blue, except when selected molecules are highlighted in green. Molecules of DMSO and CHCl<sub>3</sub> are omitted for clarity. (a) View showing how hydrogen bonding of molecules of compound **7a** according to motif **I** generates chains and how the chains are connected to produce layers by hydrogen bonds of type **III** and additional interactions. Chains in the upper level are shown in normal colors and chains in the lower level are highlighted in green. (b) View along the chains showing the relationship between the upper and lower chains in a single layer.

standard patterns of self-association. For this reason, we avoided using TFA in subsequent efforts to crystallize analogous DAT-substituted phenanthrolines **7a–9a**.

**Structure of Crystals of DAT-Substituted 1,10-Phenanthroline 7a.** Crystals of DAT-substituted phenanthroline **7a** grown from DMSO/CHCl<sub>3</sub> were found to belong to the triclinic space group *P* $\bar{1}$  and to have the composition **7a** • 2DMSO • CHCl<sub>3</sub>. Views of the structure are presented in Figure 5, and other crystallographic data are summarized in Table 2. As expected, molecules of compound **7a** adopt a flattened conformation, with the DAT substituents lying close to the plane of the phenanthroline core (dihedral angles of 5.7° and 32.4°). As illustrated in Figure 5a, molecules of compound **7a** are connected by N–H···N(triazine) hydrogen bonds of type **I** (average distance = 2.970 Å) to form chains, which are then joined to adjacent chains by N–H···N(triazine) hydrogen bonds of type **III** (3.012 Å), as well as by additional N–H···N(pyridine) hydrogen bonds (3.010 Å) and C–H···N(pyridine) interactions involving CHCl<sub>3</sub> (C···N distance = 3.109 Å). The result is a robust corrugated layer in which each molecule is linked to four neighbors by a total of eight hydrogen bonds (Figure 5b). Adjacent layers are separated by included molecules of DMSO and CHCl<sub>3</sub>.<sup>31</sup>

**Structure of Crystals of Isomeric DAT-Substituted 1,10-Phenanthroline 8a.** Crystals of isomeric DAT-substituted phenanthroline **8a** grown from DMSO/CH<sub>2</sub>Cl<sub>2</sub> were found to belong to the triclinic space group *P* $\bar{1}$  and to have the approximate composition **38a** • 2DMSO • CH<sub>2</sub>Cl<sub>2</sub>. Views of the structure are shown in Figure 6, and other crystallographic data are presented in Table 2. The structure is composed of three crystallographically independent

TABLE 2. Crystallographic Data for Isomeric DAT-Substituted Phenanthrolines 7a-9a

	7a·2DMSO·CHCl <sub>3</sub>	38a·2DMSO·CH <sub>2</sub> Cl <sub>2</sub>	9a·2DMSO
crystallization medium	DMSO/CHCl <sub>3</sub>	DMSO/CH <sub>2</sub> Cl <sub>2</sub>	DMSO/CH <sub>2</sub> Cl <sub>2</sub>
formula	C <sub>23</sub> H <sub>27</sub> Cl <sub>3</sub> N <sub>12</sub> O <sub>2</sub> S <sub>2</sub>	C <sub>59</sub> H <sub>56</sub> Cl <sub>2</sub> N <sub>36</sub> O <sub>2</sub> S <sub>2</sub>	C <sub>22</sub> H <sub>26</sub> N <sub>12</sub> O <sub>2</sub> S <sub>2</sub>
crystal system	triclinic	triclinic	triclinic
space group	<i>P</i> $\bar{1}$	<i>P</i> $\bar{1}$	<i>P</i> $\bar{1}$
<i>a</i> (Å)	9.4341(4)	14.5409(13)	11.0524(2)
<i>b</i> (Å)	9.6042(5)	14.7369(12)	11.1745(2)
<i>c</i> (Å)	16.7333(13)	21.9376(17)	11.6989(3)
$\alpha$ (deg)	95.152(5)	84.221(4)	88.330(1)
$\beta$ (deg)	98.059(4)	82.535(4)	67.213(1)
$\gamma$ (deg)	111.604(3)	69.260(4)	76.467(1)
<i>V</i> (Å <sup>3</sup> )	1379.16(14)	4351.5(6)	1292.10(5)
<i>Z</i>	2	2	2
$\rho_{\text{calc}}$ (g cm <sup>-3</sup> )	1.623	1.096 <sup>a</sup>	1.426
<i>T</i> (K)	150	150	150
$\mu$ (mm <sup>-1</sup> )	4.848	1.590	2.263
<i>R</i> <sub>1</sub> , <i>I</i> > 2 $\sigma$ ( <i>I</i> )	0.0892	0.0646	0.0537
<i>R</i> <sub>1</sub> , all data	0.1994	0.0707	0.0570
<i>wR</i> <sub>2</sub> , <i>I</i> > 2 $\sigma$ ( <i>I</i> )	0.1831	0.1544	0.1280
<i>wR</i> <sub>2</sub> , all data	0.2195	0.1553	0.1288
independent reflections	5004	13545	4559
observed reflections [ <i>I</i> > 2 $\sigma$ ( <i>I</i> )]	3511	7919	3089

<sup>a</sup>The value of  $\rho_{\text{calc}}$  does not take into account all molecules of guests included in the structure, but only those that occupy well-located positions.

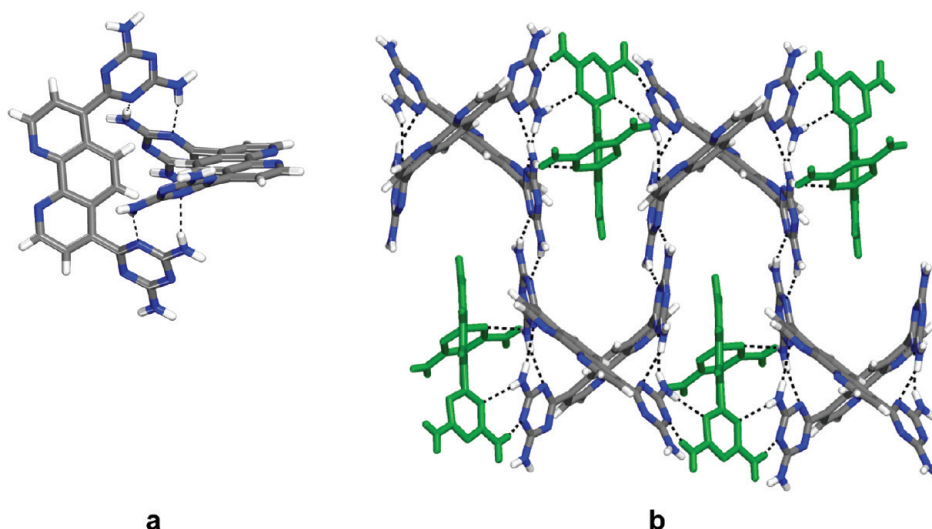


**FIGURE 6.** Views of the structure of crystals of the 3:2:1 solvate of DAT-substituted phenanthroline **8a** with DMSO and CH<sub>2</sub>Cl<sub>2</sub>. Hydrogen bonds are represented by broken lines, and carbon atoms are shown in gray, hydrogen atoms in white, and nitrogen atoms in blue. Molecules of DMSO and CH<sub>2</sub>Cl<sub>2</sub> are omitted for clarity. (a) View showing how hydrogen bonding of molecules **A** and **B** according to motif **III** generates pairs. (b) View showing how the **AB** pairs are further connected to form columns by hydrogen bonding to molecules **C**, which are shown in green.

molecules **A**, **B**, and **C**, which interact to form a complex three-dimensional hydrogen-bonded network. As expected, the 4,7-pattern of disubstitution prevents the DAT groups from lying in the plane of the phenanthroline core, and the dihedral angles lie in the range 23.9–69.3°. The structure can be considered to be built from a fundamental pair of molecules **A** and **B**, which are joined by a total of four N–H···N(triazine) hydrogen bonds of type **III** with an average distance of 3.068 Å (Figure 6a). The **AB** pairs are linked into columns along the *b* axis by intervening molecules **C**, each of which engages in a total of five intracolumn hydrogen bonds, including four of type **II** with an average distance of 3.011 Å (Figure 6b). Adjacent columns are further connected by the formation of various inter-column hydrogen bonds of types **II** and **III** involving pairs **A**<sub>2</sub> and **B**<sub>2</sub>.

**Structure of Crystals of Isomeric DAT-Substituted 1,10-Phenanthroline 9a.** Crystals of isomeric DAT-substituted phenanthroline **9a** grown from DMSO/CH<sub>2</sub>Cl<sub>2</sub> were found to belong to the triclinic space group *P* $\bar{1}$  and to have the composition **9a**·2DMSO. Figure 7 provides a view of the structure, and Table 2 summarizes other crystallographic data. In the structure, molecules of compound **9a** interact to generate a complex three-dimensional hydrogen-bonded network. As anticipated, the 5,6-pattern of disubstitution forces the DAT groups to twist significantly out the plane of the phenanthroline core, and the dihedral angles are 54° and 74°. As shown in Figure 7, molecules of compound **9a** are linked into chains aligned with the *c* axis by N–H···N(triazine) hydrogen bonds of type **III** (average distance = 2.956 Å), augmented by single N–H···N(pyridine) hydrogen bonds (3.013 Å). Adjacent chains are further connected

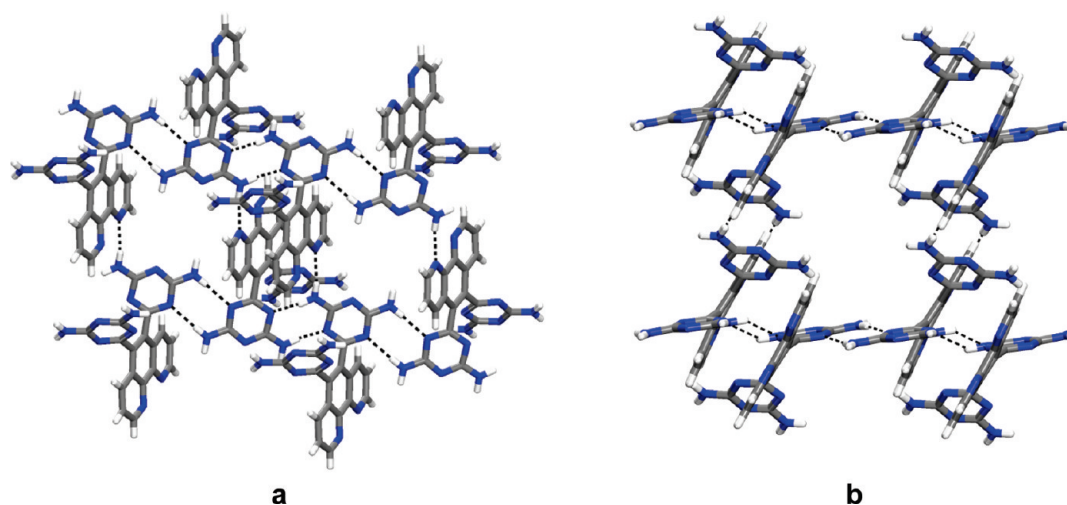


**FIGURE 7.** View of the structure of crystals of the 1:2 solvate of DAT-substituted phenanthroline **9a** with DMSO. Hydrogen bonds are represented by broken lines, and carbon atoms are shown in gray, hydrogen atoms in white, and nitrogen atoms in blue. Molecules of DMSO are omitted for clarity. The view shows how chains are formed by N–H···N(triazine) hydrogen bonds of type **III**, reinforced by single N–H···N(pyridine) hydrogen bonds. Adjacent chains are further connected by N–H···N(triazine) hydrogen bonds of type **I** to form a three-dimensional network.

by N–H···N(triazine) hydrogen bonds of type **I** (3.039 Å) to form a three-dimensional network. Each molecule of compound **9a** thereby participates in a total of seven N–H···N hydrogen bonds involving four neighbors.

## Conclusions

Previous work has established that isomeric DAT-substituted pyridines **1–3** and simple relatives tend to crystallize in foreseeable ways.<sup>8</sup> In particular, they prefer to adopt flattened conformations and to engage in approximately coplanar intermolecular hydrogen bonds of types **I–III**, which are characteristic of DAT groups.<sup>1</sup> Together, these properties ensure that molecular association is dominated by the presence of the DAT groups and favors the formation of networks that incorporate linear or planar elements such as chains, tapes, or layers.

Our present results confirm that the crystallization of more complex analogues such as DAT-substituted bipyridines **4a–6a** and phenanthrolines **7a–9a** normally follows similar patterns, as expected. Again, flattened conformations are adopted in all cases except those of compounds **8a** and **9a**, which have patterns of substitution that prevent the DAT groups from lying in the plane of the phenanthroline core. Nevertheless, DAT groups in all compounds **4a–9a** continue to play a dominant role in directing molecular association according to standard motifs **I–III** or related patterns. Notable exceptions to this generalization arise when crystallization is carried out in media with components such as TFA, which can protonate the DAT groups and thereby prevent them from engaging in normal self-association.

Detailed comparison of the hydrogen-bonded networks generated by simple DAT-substituted pyridines **1–3** with those of more complex analogs **4a–9a** reveals a series of predictable differences in connectivity and architecture. In particular, compounds **1–3** contain a single DAT group per molecule, whereas analogs **4a–9a** incorporate two DAT groups per molecule and can thereby form structures

in which each molecule is connected to more neighbors by a larger number of hydrogen bonds. As a result, compounds **4a–9a** are able in many cases to generate potentially robust architectures maintained by three-dimensional networks of hydrogen bonds, whereas simpler analogues **1–3** are typically limited to connectivity in one or two dimensions.<sup>8</sup>

In addition, the structures of simple compounds **1–3** differ predictably from those of more complex analogues **4a–9a** in the efficiency of molecular packing. Compounds with multiple substituents that engage in strong directional intermolecular interactions cannot normally form periodic structures in which the interactions and packing are optimized simultaneously.<sup>1</sup> As a result, such compounds tend to form open networks with significant volumes occupied by molecules of solvent or other guests. This pattern of behavior is nicely illustrated by the structures of compounds **1–3**, **4a–6a**, and **7a–9a**. Simple compounds **1–3**, in which directional interactions are derived primarily from a single DAT group, can crystallize without excessive constraints, and they form compact, guest-free structures in four out of six cases studied, with no structure showing a molar guest:host ratio larger than 1. In contrast, more complex analogues **4a–9a**, in which directional interactions are approximately doubled, fail to generate guest-free structures in any of the seven cases examined, and the molar guest/host ratios range up to 7.

Our work identifies DAT-substituted bipyridines **4a–6a** and phenanthrolines **7a–9a** as potentially rich sources of new supramolecular chemistry and describes how they can be made. The compounds feature well-defined molecular topologies and an ability to engage extensively in strong intermolecular interactions, directed both by hydrogen bonding and chelation of metals. Our initial structural studies have confirmed that the DAT groups of compounds **4a–9a** can play a dominant role in directing crystallization by self-associating according to standard hydrogen-bonding motifs **I–III**. This observation suggests that the sites of hydrogen bonding and chelation in compounds **4a–9a**

can accomplish their tasks independently and can thereby control association without mutual interference. Future studies will examine how metal complexes of compounds **4a–9a** can be formed and used to construct complex three-dimensional hydrogen-bonded networks. As a result, the present work is a promising starting point for a wide range of projects in organic and inorganic chemistry that target the design and synthesis of related ligands for the self-assembly of metal–organic materials with predetermined structures.

## Experimental Section

**General Notes.** 2,2'-Bipyridine-5,5'-dicarbonitrile (**4b**),<sup>11</sup> 4,4'-dibromo-2,2'-bipyridine (**5c**),<sup>20</sup> 2,2'-bipyridine-6,6'-dicarbonitrile (**6b**),<sup>15</sup> 3,8-dibromo-1,10-phenanthroline (**7c**),<sup>21</sup> 4,7-dibromo-1,10-phenanthroline (**8c**),<sup>22</sup> and 5,6-dibromo-1,10-phenanthroline (**9c**)<sup>23</sup> were prepared by methods reported previously. The syntheses of dinitriles **5b** and **7b–9b** are described below, followed by the preparation of DAT-substituted derivatives **4a–9a**. Other chemicals were purchased from commercial sources and used without further purification.

**Syntheses of Dinitriles 5b and 7b–9b.** 2,2'-Bipyridine-4,4'-dicarbonitrile (**5b**)<sup>13–15</sup>. A stirred mixture of 4,4'-dibromo-2,2'-bipyridine (**5c**; 0.873 g, 2.78 mmol), NaCN (0.274 g, 5.59 mmol), Pd(OAc)<sub>2</sub> (0.031 g, 0.14 mmol), 1,5-bis(diphenylphosphino)pentane (0.247 g, 0.561 mmol), TMEDA (0.488 g, 4.20 mmol), and mesitylene (15 mL) was sparged with N<sub>2</sub> for 10 min and then was heated at reflux under N<sub>2</sub> for 12 h. The mixture was allowed to cool, degassed water was added, and the resulting slurry was stirred for 10 min. The slurry was filtered, and the solid was rinsed with pentane and then purified by flash chromatography (silica gel, hexane/ethyl acetate 7/3) to give 2,2'-bipyridine-4,4'-dicarbonitrile (**5b**; 0.363 g, 1.76 mmol, 63%) as a colorless solid: mp 220 °C; IR (ATR) 2238 cm<sup>-1</sup>; <sup>1</sup>H NMR (400 MHz, CDCl<sub>3</sub>) δ 8.90 (dd, 2H, <sup>5</sup>J = 0.87 Hz, <sup>3</sup>J = 4.9 Hz), 8.74 (dd, 2H, <sup>4</sup>J = 1.5 Hz, <sup>5</sup>J = 0.93 Hz), 7.62 (dd, 2H, <sup>3</sup>J = 4.9 Hz, <sup>4</sup>J = 1.5 Hz); <sup>13</sup>C NMR (100 MHz, CDCl<sub>3</sub>) δ 155.9, 150.7, 126.3, 123.5, 122.2, 116.8; HRMS (ESI) calcd for C<sub>12</sub>H<sub>6</sub>N<sub>4</sub> + H *m/e* 207.06652, found 207.06687.

**1,10-Phenanthroline-3,8-dicarbonitrile (7b).** A stirred mixture of 3,8-dibromo-1,10-phenanthroline (**7c**; 1.10 g, 3.25 mmol), NaCN (0.322 g, 6.57 mmol), Pd(OAc)<sub>2</sub> (0.036 g, 0.16 mmol), 1,5-bis(diphenylphosphino)pentane (0.291 g, 0.661 mmol), TMEDA (0.572 g, 4.92 mmol), and mesitylene (15 mL) was sparged with N<sub>2</sub> for 10 min and then was heated at reflux under N<sub>2</sub> for 12 h. The mixture was allowed to cool, degassed water was added, and the resulting slurry was stirred for 10 min. The slurry was filtered, and the solid was rinsed with pentane and then purified by flash chromatography (silica gel, hexane/ethyl acetate 1/1) to give 1,10-phenanthroline-3,8-dicarbonitrile (**7b**; 0.460 g, 2.00 mmol, 62%) as a yellow-orange solid: mp > 250 °C dec; IR (ATR) 2230 cm<sup>-1</sup>; <sup>1</sup>H NMR (400 MHz, CDCl<sub>3</sub>) δ 9.44 (d, 2H, <sup>4</sup>J = 2.0 Hz), 8.71 (d, 2H, <sup>4</sup>J = 2.0 Hz), 8.03 (s, 2H); <sup>13</sup>C NMR (100 MHz, CDCl<sub>3</sub>) δ 151.3, 146.6, 140.9, 128.5, 127.9, 116.3, 110.1; HRMS (ESI) calcd for C<sub>14</sub>H<sub>6</sub>N<sub>4</sub> + H *m/e* 231.0665, found 231.0662.

**1,10-Phenanthroline-4,7-dicarbonitrile (8b).**<sup>18</sup> Compound **8b** was prepared in 60% yield by the method described above for making isomer **7b**. Crystallization from CHCl<sub>3</sub>/MeCN provided yellow blocks: mp > 250 °C dec; IR (ATR) 2105 cm<sup>-1</sup>; <sup>1</sup>H NMR (400 MHz, CDCl<sub>3</sub>) δ 9.43 (d, 2H, <sup>3</sup>J = 4.4 Hz), 8.46 (s, 2H), 8.08 (d, 2H, <sup>3</sup>J = 4.4 Hz); <sup>13</sup>C NMR (100 MHz, CDCl<sub>3</sub>) δ 151.2, 146.4, 127.8, 127.4, 126.3, 119.8, 115.4; HRMS (ESI) calcd for C<sub>14</sub>H<sub>6</sub>N<sub>4</sub> + H *m/e* 231.0665, found 231.0677.

**1,10-Phenanthroline-5,6-dicarbonitrile (9b).** Compound **9b** was prepared in 52% yield by the method described above for

making isomer **7b**. Crystallization from CH<sub>2</sub>Cl<sub>2</sub>/MeCN provided red blocks: mp > 250 °C (dec); IR (ATR) 2231 cm<sup>-1</sup>; <sup>1</sup>H NMR (400 MHz, CDCl<sub>3</sub>) δ 9.46 (dd, 2H, <sup>3</sup>J = 4.3 Hz, <sup>4</sup>J = 1.7 Hz), 8.77 (dd, 2H, <sup>3</sup>J = 8.3 Hz, <sup>4</sup>J = 1.7 Hz), 7.97 (dd, 2H, <sup>3</sup>J = 8.3 Hz, <sup>3</sup>J = 4.3 Hz); <sup>13</sup>C NMR (100 MHz, CDCl<sub>3</sub>) δ 154.8, 147.0, 135.3, 126.0, 125.7, 117.1, 114.0; HRMS (ESI) calcd for C<sub>14</sub>H<sub>6</sub>N<sub>4</sub> + H *m/e* 231.0665, found 231.0658.

**Syntheses of DAT-Substituted Bipyridines 4a–6a and Phenanthrolines 7a–9a.** 6,6'-(2,2'-Bipyridine-5,5'-diyl)bis(1,3,5-triazine-2,4-diamine) (**4a**). A mixture of 2,2'-bipyridine-4,4'-dicarbonitrile (**4b**; 0.673 g, 3.26 mmol),<sup>11</sup> dicyandiamide (0.688 g, 8.18 mmol), and KOH (0.202 g, 3.60 mmol) in 2-methoxyethanol (25 mL) was heated at reflux for 12 h. The mixture was allowed to cool, and precipitated solids were then separated by filtration, washed with hot water, rinsed with MeOH, and dried under vacuum to provide DAT-substituted bipyridine **4a** (1.10 g, 2.94 mmol, 90%) as a nearly colorless solid: mp > 350 °C; IR (ATR) 3459, 3327, 3153, 1662, 1633, 1525, 1442, 1394, 1359, 857 cm<sup>-1</sup>; <sup>1</sup>H NMR (400 MHz, DMSO-*d*<sub>6</sub>) δ 9.47 (d, 2H, <sup>4</sup>J = 2.0 Hz), 8.69 (dd, 2H, <sup>3</sup>J = 8.3 Hz, <sup>4</sup>J = 2.0 Hz), 8.58 (d, 2H, <sup>3</sup>J = 8.3 Hz), 6.929 (br s, 8H); <sup>13</sup>C NMR (100 MHz, DMSO-*d*<sub>6</sub>) δ 169.4, 168.2, 157.4, 149.8, 137.2, 133.8, 121.5; HRMS (ESI) calcd for C<sub>16</sub>H<sub>14</sub>N<sub>12</sub> + H *m/e* 375.1537, found 375.1547.

**6,6'-(2,2'-Bipyridine-4,4'-diyl)bis(1,3,5-triazine-2,4-diamine) (5a).** Compound **5a** was prepared from 2,2'-bipyridine-4,4'-dicarbonitrile (**5b**) in 85% yield by the method described above for making analogue **4a**: mp > 350 °C; IR (ATR) 3463, 3317, 3119, 1643, 1531, 1396, 809 cm<sup>-1</sup>; <sup>1</sup>H NMR (400 MHz, DMSO-*d*<sub>6</sub>) δ 9.27 (s, 2H), 8.86 (d, 2H, <sup>3</sup>J = 4.9 Hz), 8.17 (dd, 2H, <sup>3</sup>J = 4.9 Hz), 7.02 (br d, 8H); <sup>13</sup>C NMR (100 MHz, DMSO-*d*<sub>6</sub>) δ 169.5, 168.4, 156.6, 150.8, 146.7, 122.9, 119.5; HRMS (ESI) calcd for C<sub>16</sub>H<sub>14</sub>N<sub>12</sub> + H *m/e* 375.1537, found 375.1538.

**6,6'-(2,2'-Bipyridine-6,6'-diyl)bis(1,3,5-triazine-2,4-diamine) (6a).** Compound **6a** was prepared from 2,2'-bipyridine-6,6'-dicarbonitrile (**6b**)<sup>15</sup> in 90% yield by the method described above for making analogue **4a**: mp > 350 °C; IR (ATR) 3479, 3357, 3146, 1617, 1538, 1403, 805 cm<sup>-1</sup>; <sup>1</sup>H NMR (400 MHz, DMSO-*d*<sub>6</sub>) δ 8.55 (d, 2H, <sup>3</sup>J = 7.8 Hz), 8.23 (d, 2H, <sup>3</sup>J = 7.6 Hz), 8.11 (t, 2H, <sup>3</sup>J = 7.8 Hz), 6.92 (br d, 8H); <sup>13</sup>C NMR (100 MHz, DMSO-*d*<sub>6</sub>) δ 171.3, 168.5, 155.8, 155.7, 138.6, 124.6, 123.1; HRMS (ESI) calcd for C<sub>16</sub>H<sub>14</sub>N<sub>12</sub> + H *m/e* 375.1537, found 375.1537.

**6,6'-(1,10-Phenanthroline-3,8-diyl)bis(1,3,5-triazine-2,4-diamine) (7a).** Compound **7a** was prepared from 1,10-phenanthroline-3,8-dicarbonitrile (**7b**) in 89% yield by the method described above for making analogue **4a**: mp > 350 °C; IR (ATR) 3325, 3165, 1634, 1531, 1391 cm<sup>-1</sup>; <sup>1</sup>H NMR (400 MHz, DMSO-*d*<sub>6</sub>) δ 9.88 (s, 2H), 9.20 (s, 2H), 8.18 (s, 2H), 7.01 (br s, 8H); <sup>13</sup>C NMR (100 MHz, DMSO-*d*<sub>6</sub>) δ 169.1, 167.8, 149.7, 147.0, 135.9, 132.3, 128.9, 128.2; HRMS (ESI) calcd for C<sub>18</sub>H<sub>14</sub>N<sub>12</sub> + H *m/e* 399.1537, found 399.1537.

**6,6'-(1,10-Phenanthroline-4,7-diyl)bis(1,3,5-triazine-2,4-diamine) (8a).** Compound **8a** was prepared from 1,10-phenanthroline-4,7-dicarbonitrile (**8b**) in 85% yield by the method described above for making analogue **4a**: mp > 350 °C; IR (ATR) 3330, 3150, 1532 cm<sup>-1</sup>; <sup>1</sup>H NMR (400 MHz, DMSO-*d*<sub>6</sub>) δ 9.20 (d, 2H, <sup>3</sup>J = 4.4 Hz), 8.66 (s, 2H), 8.03 (d, 2H, <sup>3</sup>J = 4.4 Hz), 7.03 (br s, 8H); <sup>13</sup>C NMR (400 MHz, DMSO-*d*<sub>6</sub>) δ 172.4, 167.9, 150.4, 147.0, 144.3, 126.0, 125.5, 123.8; HRMS (ESI) calcd for C<sub>18</sub>H<sub>14</sub>N<sub>12</sub> + H *m/e* 399.1537, found 399.1543.

**6,6'-(1,10-Phenanthroline-5,6-diyl)bis(1,3,5-triazine-2,4-diamine) (9a).** Compound **9a** was prepared from 1,10-phenanthroline-5,6-dicarbonitrile (**9b**) in 20% yield by the method described above for making analogue **4a**: mp > 350 °C; IR (ATR) 3120, 1629, 1540 cm<sup>-1</sup>; <sup>1</sup>H NMR (400 MHz, DMSO-*d*<sub>6</sub>) δ 9.12 (d, 2H, <sup>3</sup>J = 3.0 Hz), 8.36 (d, 2H, <sup>3</sup>J = 8.3 Hz), 7.75 (dd, 2H, <sup>3</sup>J = 3.0 Hz, <sup>3</sup>J = 8.0 Hz), 6.66 (br s, 8H); <sup>13</sup>C NMR (100 MHz, DMSO-*d*<sub>6</sub>) δ 172.7, 167.5, 150.9, 146.0, 136.0, 134.0, 127.1,

124.1; HRMS (ESI) calcd for  $C_{18}H_{14}N_{12} + H$   $m/e$  399.1537, found 399.1535.

**Crystallization of DAT-Substituted Bipyridines 4a–6a and Phenanthrolines 7a–9a.** Crystals used for structural studies by X-ray diffraction were grown at 25 °C in the following ways. DAT-substituted bipyridine **4a** was crystallized by allowing vapors of MeOH to diffuse into a saturated solution in DMSO. In addition, crystals of compound **4a** and isomer **5a** were obtained by allowing vapors of water to diffuse into solutions in TFA (~5 mg/mL). Crystals of DAT-substituted bipyridine **6a** were grown by allowing vapors of  $CH_2Cl_2$  to diffuse into a saturated solution in DMSO. Similarly, DAT-substituted phenanthrolines **7a**, **8a**, and **9a** were crystallized by allowing vapors of  $CHCl_3$  (compound **7a**) or  $CH_2Cl_2$  (compounds **8a** and **9a**) to diffuse into saturated solutions in DMSO.

**Analysis of the Structures of DAT-Substituted Bipyridines 4a–6a and Phenanthrolines 7a–9a by X-ray Crystallography.** Crystallographic data were collected using a Bruker Microstar diffractometer with Cu  $K\alpha$  radiation. The structures were solved by direct methods using SHELXS-97, and non-hydrogen atoms were refined anisotropically with SHELXL-97.<sup>32</sup> Hydrogen atoms were first located from difference Fourier

maps, and then their positions were recalculated, using standard values of distances and angles, before refining them as riding atoms. In the structures of compounds **4a** and **6a** crystallized from TFA, the positions of hydrogen-bonded atoms of hydrogen derived from TFA could not be determined reliably. These atoms were assigned to the nitrogen atom of the hydrogen-bond acceptor, and a full proton transfer was assumed to occur. In the case of crystals of compound **8a** grown from DMSO/ $CH_2Cl_2$ , only part of the included molecules of solvent could be resolved. The SQUEEZE option of the program PLATON<sup>33</sup> was used to eliminate the contribution of included molecules that were highly disordered, thereby giving a final model for the most ordered part of the structure.

**Acknowledgment.** We are grateful to the Natural Sciences and Engineering Research Council of Canada, the Ministère de l'Éducation du Québec, the Canada Foundation for Innovation, the Canada Research Chairs Program, and Université de Montréal for financial support.

**Supporting Information Available:** Additional crystallographic details (including thermal atomic displacement ellipsoid plots, tables of structural data in CIF format, and supplementary figures), as well as  $^1H$  and  $^{13}C$  NMR spectra for all new compounds. This material is available free of charge via the Internet at <http://pubs.acs.org>.

(32) Sheldrick, G. M. *Acta Crystallogr.* **2008**, *A64*, 112–122.

(33) Spek, A. L. *PLATON, A Multipurpose Crystallographic Tool*; Utrecht University: Utrecht, The Netherlands, 2001. van der Sluis, P.; Spek, A. L. *Acta Crystallogr.* **1990**, *A46*, 194–201.